Chaotic behavior analysis of two-bar trusses under inelastic effects through Lyapunov exponents

Gustavo B. Barbosa[1], William L. Fernandes[2], Marcelo Greco[1]

[1]*Dept. of Structural Engineering, Federal University of Minas Gerais*
6627 Antônio Carlos Ave., 31270-901, Belo Horizonte, State of Minas Gerais, Brazil
gustavo-botelho@ufmg.br, mgreco@dees.ufmg.br
[2]*Dept. of Civil Engineering, Pontifical Catholic University of Minas Gerais*
1200 Afonso Vaz de Melo Ave., 31270-901, Belo Horizonte, State of Minas Gerais, Brazil
wlfernandes13@gmail.com

Abstract. The advancement of engineering structures is increasingly leading to slender and light elements that require more complex analysis. Instability problems are frequently observed in such situations, and their study is of fundamental importance. Numerical methods are commonly used in those analyses. It is proposed in this work to use a variation of the Finite Element Method, called for a Positional Formulation (PFEM), with the advantage that the geometric nonlinearity is naturally incorporated into the method. In terms of physical nonlinearity, a mixed-hardening model is used in the Formulation. The dynamic analysis is carried out by Newmark's method of integration in the time domain, and the Newton-Raphson Method is used to solve the equations of equilibrium. Also, Lyapunov exponents are employed to determine the regions where the chaotic behavior occurs. One example of a two-truss bar is used to verify the effectiveness of the implemented formulation and the influence of inelasticity in the chaotic behavior. The analysis is done by different values of the initial conditions, since chaos is sensitive to such variations.

Keywords: Mixed-hardening model, Lyapunov exponents, Positional Finite Element Method, Nonlinear analysis.

1 Introduction

The advancement of engineering structures is increasingly leading to slender and light elements that require more complex analysis. Instability problems are frequently observed in such situations and chaotic behavior is one of them. The term chaos is commonly used to describe seemingly random behavior (Hilborn [1]). From a mathematical point of view, it is associated with a phenomenon that has a sensitive dependence on initial conditions (Layek [2]). The study of such phenomena is closely linked with nonlinear systems (Hilborn [1]), which describes, therefore, nonlinear oscillation phenomena. Thus, the stability/instability of a system is only properly assessed from the dynamic analysis point of view. There are many ways to determine the existence of chaotic behavior and its applications in structural engineering are wide. Poddar et al. [3] make use of Poincaré Maps in the study of elastoplastic beams with chaotic behavior, where the influence of geometric and material nonlinearity in the evolution of the system's behavior is explained. Thomsen [4] addresses chaotic vibrations of non-shallow arches through Lyapunov exponents, Poncaré sections, and frequency spectra. Karagiozov and Karagiozova [5] also uses Poincaré Maps and Lyapunov exponents to determine the sensitivity of initial conditions to the vibration response of an elastoplastic column. Other works that can be cited in this field: Yang et al. [6], Luo et al. [7].

To obtain the answers to such problems and then analyze the nature of the behavior, numerical methods of PDEs solution are used, more commonly performed by the finite element method. There are many variations of the method, including positional formulation. Such a formulation was presented by Coda [8] and Greco [9], and used for many purposes. Focusing on studies involving instability in slender elements, it is possible to cite Kzam [10] and Fernandes et al. [11], the latter dealing with nonlinear oscillations. In the present work, positional formulation and Lyapunov exponents were used to characterize the nature of the evolution of vibrations.

2 Finite Element Method: Positional Formulation (PFEM)

The traditional way of solving differential equations in engineering problems is the Finite Element Method based on nodal displacements. In Coda [8] a formulation based on nodal positions is presented, which can be related to displacements by the eq. (1):

$$\mathbf{u} = \mathbf{X} - \mathbf{X_0}, \;\; \dot{\mathbf{u}} = \dot{\mathbf{X}} \text{ and } \ddot{\mathbf{u}} = \ddot{\mathbf{X}}, \tag{1}$$

where $\mathbf{u}$ is the nodal displacement, $\mathbf{X_0}$ is the initial nodal position vector, and $\mathbf{X}$ is the nodal position at any instant, $\dot{()}$ and $\ddot{()}$ represents velocity and acceleration in each formulation, respectively.

Furthermore, the method adopts the Total Lagrangian description, the Bernoulli-Euler kinematics, and the equilibrium is described through the Principle of Total Stationary Energy. The formulation still has, in an intrinsic way, geometric nonlinearity due to the use of the Newton-Raphson Method for the equilibrium solution.

Greco [9] adds to the Formulation the elastoplastic behavior in the material, making use of the mixed hardening model. The author also included dynamic behavior considering the Newmark Method for the dynamic analysis.

The formulation part of the energy functional that contains all the parts that contribute to the determination of the system balance is given by eq. (2):

$$\Pi = U_t + P + K_c + K_a, \tag{2}$$

where U_t, is the potential energy, P, work done by external forces, K_c, kinetic energy, and K_a, damping, are given by equations (eq. (3)-eq. (6)) that follows:

$$U_t = \frac{1}{2}\int_V E(\varepsilon^2 - \varepsilon\varepsilon_p)dV, \tag{3}$$

$$P = -\mathbf{F}\mathbf{X}, \tag{4}$$

$$K_c = \int_V \frac{\rho}{2}\dot{\mathbf{X}}^2 dV, \tag{5}$$

$$K_a = \int_V c_m \rho \mathbf{X}\dot{\mathbf{X}} dV - \int_V \int_{X_k} c_m \rho \frac{\mathbf{X}\dot{\mathbf{X}}}{\dot{\mathbf{X}}} dX_k dV, \tag{6}$$

where in eq. (3) E is Young modulus, ε is the engineering strain, and plastic strain ε_p is given by the hardening model. $\mathbf{F}$ is a set of external forces, $\mathbf{X}$ represents a set of independent coordinates of a given nodal, and $\dot{\mathbf{X}}$ is a set of nodal velocity. Yet, c_m and ρ represent the coefficient of damping and specific mass, respectively. Furthermore, the strain energy is given in terms of reference volume (V), due to the Total Langrangian description.

The mixed-hardening model adopted in the formulation is described by the evolution law of the elastic limit by:

$$\Phi(\sigma, \sigma_y, K, H) = |\sigma - q| - (\sigma_y + K\alpha) \;\text{ and }\; \Phi \leq 0, \tag{7}$$

where σ is the stress, σ_y yield stress, α and $q(H)$ are internal variables which represent, respectively, the plastic deformation evolution and the translation of the center of the elastic interval. K is the hardening modulus and H

is the kinematic modulus. Furthermore, when $K = H = 0$, the perfect-plasticity model is obtained, and $H = 0$ gives the isotropic-hardening model. And, Φ greater than zero indicate plastic deformation. The solution for plastic deformation is carried out using numerical integration according to returning-mapping presented by Simo and Hughes [12].

In the formulation presented by Greco [9], the Rayleigh's proportional mass dumping is used. Yet, the mass is considered discrete and the terms related to rotation are neglected, which explains the zeros on the diagonal of the matrix (eq. (8)). Hence, in the right-side of the same eq. (8), the coefficient of damping can be rewritten in a matrix form.

$$\mathbf{M} = \frac{\rho AL}{2} diag \begin{bmatrix} 1 & 1 & 0 & 1 & 1 & 0 \end{bmatrix}, \quad \mathbf{C} = 2c_m \mathbf{M}. \tag{8}$$

Through the eq. (6) and eq. (8), the damping energy can be described in terms of:

$$K_a = \mathbf{C}\mathbf{X}\dot{\mathbf{X}} - \mathbf{C}\int_{X_k} \frac{\mathbf{X}\dot{\mathbf{X}}}{\dot{\mathbf{X}}} dX_k dV. \tag{9}$$

The functional described in eq. (2) should be minimized in order to obtain the equilibrium of the system through the Principle of Stationary Total Potential Energy. Then, the derivative of K_a and K_c in relation to nodal position is:

$$\frac{\partial K_a}{\partial X_k} = \sum_{i=1}^{DOF} c_{m_i} \left(\dot{X}_i + X_i \frac{\partial \dot{X}_i}{\partial t} \frac{\partial t}{\partial X_k} - \frac{\dot{X}_i \ddot{X}_i}{\dot{X}} \right) \delta_{ik}, \tag{10}$$

$$\frac{\partial K_c}{\partial X_k} = \sum_{i=1}^{DOF} m_i \dot{X}_i \ddot{X}_i \frac{1}{\ddot{X}_i} \delta_{ik} = \sum_{i=1}^{DOF} m_k \ddot{X}_k, \tag{11}$$

where the δ_{ik} represents the Kronecker delta. Moreover, the development of this derivative is given in detail by Greco [9].

Using eq. (10) and eq. (11), also noting that the derivate of eq. (4) is trivial, the equation of motion can be represented as follows:

$$\frac{\partial \Pi}{\partial X} = \frac{\partial U_t}{\partial X} - \mathbf{F} + \mathbf{M}\ddot{\mathbf{X}} + \mathbf{C}\dot{\mathbf{X}} = 0, \tag{12}$$

where can be observed there is a dependence of time (t) and nodal position vector ($\mathbf{X}$).

2.1 Description of numerical integration

To perform time derivation using Newmark Method it is necessary to rewrite eq. (12) for the current time $t + \Delta t$, as:

$$\left.\frac{\partial \Pi}{\partial X}\right|_{t+\Delta t} = \left.\frac{\partial U_t}{\partial X}\right|_{t+\Delta t} - \mathbf{F}_{t+\Delta t} + \mathbf{M}\ddot{\mathbf{X}}_{t+\Delta t} + \mathbf{C}\dot{\mathbf{X}}_{t+\Delta t} = 0, \tag{13}$$

which represents equation of motion in a discrete form.

Through the Newmark Method for the positional formulation, it is possible to express

$$\mathbf{X}_{t+\Delta t} = \mathbf{X}_t + \Delta t \dot{\mathbf{X}}_t + \Delta t^2 \left[\left(\frac{1}{2} - \beta \right) \ddot{\mathbf{X}}_t + \beta \ddot{\mathbf{X}}_{t+\Delta t} \right], \; \dot{\mathbf{X}}_{t+\Delta t} = \dot{\mathbf{X}}_t + \Delta t(1-\gamma)\ddot{\mathbf{X}}_t + \gamma \Delta t \ddot{\mathbf{X}}_{t+\Delta t}, \quad (14)$$

and using eq. (13) in order to isolate $\ddot{\mathbf{X}}_0$ together with eq. (1) and eq. (14) the equation of positional acceleration in $t + \Delta t$ is provided:

$$\ddot{\mathbf{X}}_{t+\Delta t} = \frac{\mathbf{X}_{t+\Delta t}}{\beta \Delta t^2} - \frac{\mathbf{X}_t}{\beta \Delta t^2} - \frac{\dot{\mathbf{X}}_t}{\beta \Delta t} - \left(\frac{1}{2\beta} - 1 \right) \ddot{\mathbf{X}}_t, \quad (15)$$

then, returning in eq. (13), yields the following equation:

$$\frac{\partial \Pi}{\partial \mathbf{X}}\Big|_{t+\Delta t} = \frac{\partial U_t}{\partial \mathbf{X}}\Big|_{t+\Delta t} - \mathbf{F}_{t+\Delta t} + \frac{\mathbf{M}\ddot{\mathbf{X}}_{t+\Delta t}}{\beta \Delta t^2} \mathbf{X}_{t+\Delta t} - \mathbf{M}\mathbf{Q}_t + \mathbf{C}\mathbf{R}_t + \frac{\gamma \mathbf{C}\dot{\mathbf{X}}_{t+\Delta t}}{\beta \Delta t} \mathbf{X}_{t+\Delta t} - \gamma \Delta t \mathbf{C}\mathbf{Q}_t = 0, \quad (16)$$

with $\mathbf{Q}_t$ and $\mathbf{R}_t$ containing contributions of the variables in the previous time instant. Moreover, these two vectors are given by the following equations:

$$\mathbf{Q}_t = \frac{\mathbf{X}_t}{\beta \Delta t^2} + \frac{\dot{\mathbf{X}}_t}{\beta \Delta t} + \left(\frac{1}{2\beta} - 1 \right) \ddot{\mathbf{X}}_t, \quad \mathbf{R}_t = \dot{\mathbf{X}}_t + \Delta t(1-\gamma)\ddot{\mathbf{X}}_t. \quad (17)$$

Finally, applying Newton-Raphson Method in eq. (16), one obtains:

$$\frac{\partial^2 \Pi}{\partial \mathbf{X}^2}\Big|_{t+\Delta t} = \nabla g(\mathbf{X}_0) = \frac{\partial U_t}{\partial \mathbf{X}}\Big|_{t+\Delta t} + \frac{\mathbf{M}}{\beta \Delta t^2} + \frac{\gamma \mathbf{C}}{\beta \Delta t}, \quad (18)$$

that define the Hessian matrix for the dynamic problem. Furthermore, for consistent notation, the $\mathbf{X}_0$ concerns the initial position vector.

3 Chaos and Lyapunov exponents

In systems with nonlinear oscillations, chaotic behavior is possible. Despite the apparent randomness of the phenomenon, it is possible to describe a given system through differential equations (Hilborn [1]). A system is stable if a small variation in initial conditions leads to a small variation in response (Bažant and Cedolin [13]). Thus, it is said that chaotic behavior is characterized by sensitivity to initial conditions. To determine the stability of a system and check if chaotic behavior occurs there are several tools, as seen in Parker and Chua [14]. In the present work, Lyapunov exponents are used, which are briefly described below.

Lyapunov exponents are parameters used to determine the stability of a system of any type, including chaotic systems (Parker and Chua [14]). These exponents can be determined, among other ways, by data from a one-dimensional time series (Hilborn [1]). Thus, assuming equality between time intervals τ, a difference between sequences of n-order is expressed by:

$$t_n - t_0 = n\tau, \quad d_n = |x(t_{j+n}) - x(t_{i+n})|. \quad (19)$$

Also, assuming that the system presents exponential evolution, as eq. (20):

$$d_n = d_0 \mathrm{e}^{\lambda_1 n}, \quad (20)$$

and then the first Lyapunov exponent is obtained by the left term of eq. (21):

$$\lambda_1 = \frac{1}{n} \ln \left(\frac{d_n}{d_0} \right), \quad \lambda_2 = \frac{1}{n} \log_2 \left(\frac{d_n}{d_0} \right). \tag{21}$$

It is also possible to express the same parameter in terms of no longer the natural logarithm but of $\log_2$ (right-side-term of eq. (21)), representing the loss of information contained in the initial value of the series.

Thus, $\lambda_{1,2} > 0$ express chaotic behavior, i.e, trajectories diverge exponentially. On the other hand, $\lambda_{1,2} < 0$, trajectories converge exponentially, indicating stability, and if $\lambda_{1,2} = 0$, the system does not evolve for any of the cases mentioned.

Hilborn [1] highlights the consequence of the hypothesis that the evolution of differences is exponential. The author recommends analyzing the graphs of the natural logarithm of the difference d_n versus the index n. If the divergence is exponential, the points will be close to, or on a straight line whose slope is the Lyapunov Exponent. Otherwise, then the Exponent is meaningless in that range.

Also according to Hilborn [1], it is possible to write the exponents in such a way as to reduce the noise of the data, in terms of an average exponent, in the form:

$$\lambda_1^{\text{aver}} = \frac{1}{N} \sum_{i=1}^{N} \lambda_1(x(t_i)), \quad \lambda_2^{\text{aver}} = \frac{1}{N} \sum_{i=1}^{N} \lambda_2(x(t_i)), \tag{22}$$

for a representative value, the author recommends N between 30 and 40, where N is the number of representative exponents.

4 Example: two-bars truss under harmonic load

It is intended to validate the proposal formulation using a relationship between the initial conditions, inelasticity, and Lyapunov exponents for a two-bar truss with pinned ends (Fig. 1), submitted to a harmonic load ($F_0 = 4000\,N$, $\omega = 57\,rad/s$). The geometrical and physical properties are $L = 10\,m$, $h = 0.20\,m$, $A = 29.14\,cm^2$, $I = 778.3\,cm^4$, $E = 199.9\,GPa$, and $\rho = 7849\,kgf/m^3$. The initial velocity conditions are 0.0, $0.001\,m/s$, and $0.005\,m/s$. The Newmark scheme ($\gamma = 0.50$; $\beta = 0.25$; $\Delta t = 10^{-3}\,s$) is used, without damping, and one finite element per bar. Four material conditions are considered: elastic model, elastic-perfectly-plastic model ($\sigma_y = 130\,MPa$), isotropic model ($\sigma_y = 130\,MPa$; $K = 19.99\,GPa$), and mixed-hardening model ($\sigma_y = 130\,MPa$; $K = 19.99\,GPa$; $H = 1.999\,MPa$).

Time-history results of the present work have good agreement with SAP2000 (Fig. 1e). The fundamental natural frequency obtained was $57.0046\,rad/s$ (present work, Subspace Iteration Method) and $57.011\,rad/s$ (SAP2000). A small change in the initial velocity $\dot{X}(0)$ leads to a significant change in response for $t \sim 2\,s$ (0.0 to $0.001\,m/s$) and $t \sim 2.2\,s$ ($0.001\,m/s$ to $0.005\,m/s$) according to Fig. 1b. The system presents dynamical snap-through at $t \sim 1.3\,s$. The isotropic model (Fig. 1c) and mixed-hardening model (Fig. 1d) show similar behavior for $\dot{X}(0) = 0.001\,m/s$ and $\dot{X}(0) = 0.005\,m/s$, but the snap-through occurs first for the isotropic model at condition $\dot{X}(0) = 0.0$. For the elastic-perfectly plastic model (Fig. 1a) there is no visible divergence between the responses.

Figure 2 shows the variation of the divergence $\mathbf{d}^{(i)}(t)$ between responses. The average Lyapunov Exponents are determined in regions of positive slope (average line) for each case. The elastic-perfectly-plastic (Fig. 2d) response differs from other cases presenting small variations for $\mathbf{d}^{(1)}(t)$ and $\mathbf{d}^{(2)}(t)$.

The time intervals, and Lyapunov exponents are indicated in Table 1. All cases present an increase of the exponents when the initial velocity condition also increases. The mixed-hardening model shows the largest loss of information about the initial conditions ($11.087 \cdot 10^{-3}\,bits/s$). The elastic-perfectly-plastic model presents the lowest values in a later time interval compared to other cases.

5 Conclusion

In this work, the influence of inelasticity on the chaotic behavior of the two-bar truss, subjected to a harmonic load, is evaluated using Lyapunov exponents. The Positional Finite Element Method formulation with nonlinear geometric and inelasticity present a good agreement with SAP2000 (classical FEM). The inclusion of inelasticity

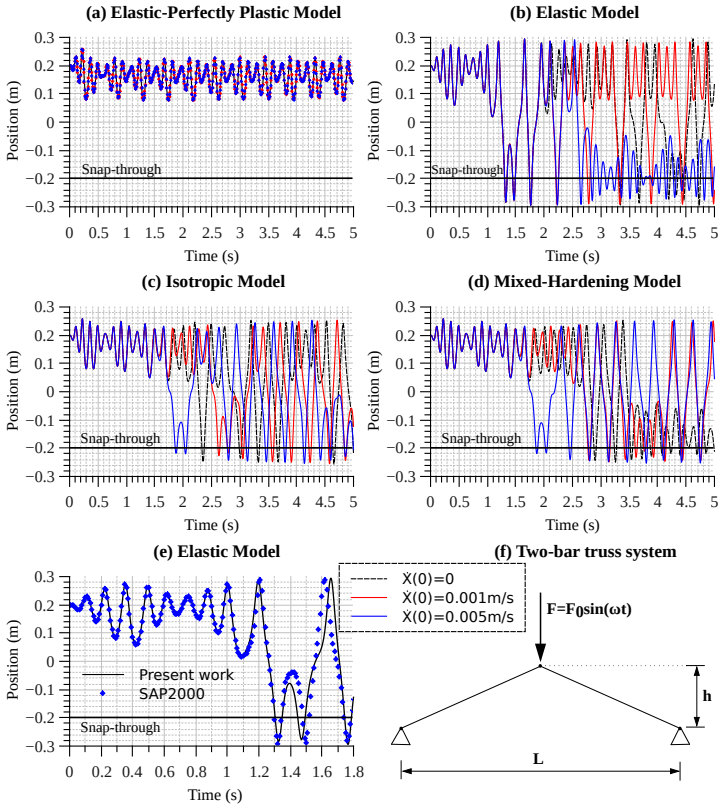

Figure 1. Positions (central node) vs. time for different initial velocity conditions and material models

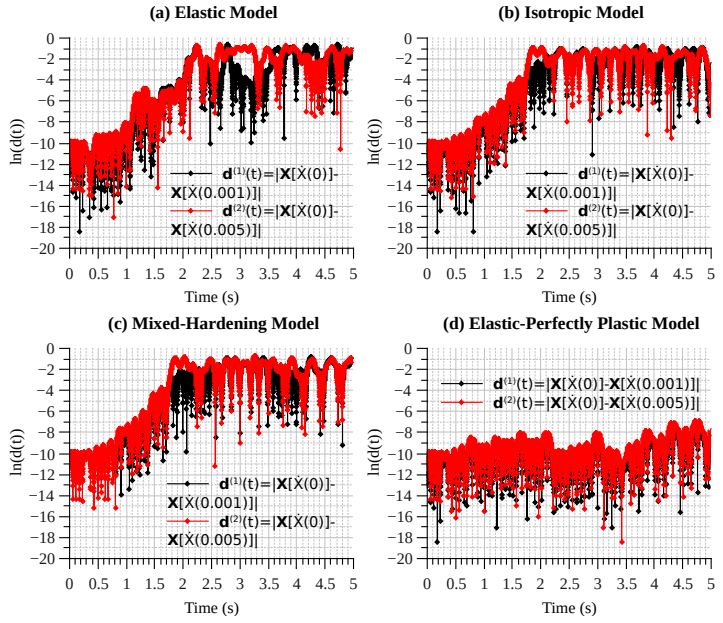

Figure 2. Divergence $\mathbf{d}^{(i)}(t)$ vs. time for material models

(isotropic and mixed-hardening models) caused an increase of the Lyapunov exponents, with a small decrease of the time interval for the two-bar truss. Furthermore, the mixed-hardening model presented the highest Lyapunov exponents, indicating a higher level of instability. It can also be seen in the Table 1 that the mixed model has a greater degree of instability. The energy dissipation along analysis reduced the chaotic behavior of the truss for the elastic-perfectly plastic model, avoiding the snap-through and decreasing the Lyapunov exponents.

Table 1. Lyapunov Exponents for material models and time intervals

Parameter (10^{-3})	Elastic $(0.5\,s - 2.2\,s)$	Isotropic hardening $(0.5\,s - 1.8\,s)$	Mixed-hardening $(0.8\,s - 2.0\,s)$	Elastic-perfect-plastic $(3.0\,s - 5.0\,s)$	Initial velocity $[m/s]$
λ_1	6.347	6.609	7.250	1.115	0 and 0.001
$\lambda_2[bits/s]$	9.157	9.535	10.460	1.609	0 and 0.001
λ_1	5.171	7.547	7.685	1.360	0 and 0.005
$\lambda_2[bits/s]$	7.460	10.887	11.087	1.962	0 and 0.005

Acknowledgements. The authors are grateful for the financial support granted by the Conselho Nacional de Desenvolvimento Científico e Tecnológico (CNPq), the Coordenação de Aperfeiçoamento de Pessoal de Nível Superior (CAPES), and the Fundação de Amparo à Pesquisa do Estado de Minas Gerais (FAPEMIG).

Authorship statement. The authors hereby confirm that they are the sole liable persons responsible for the authorship of this work, and that all material that has been herein included as part of the present paper is either the property (and authorship) of the authors, or has the permission of the owners to be included here.

References

[1] R. C. Hilborn. *Chaos and nonlinear dynamics: an introduction for scientists and engineers*. Oxford University Press on Demand, 2000.
[2] G. Layek. *An introduction to dynamical systems and chaos*. Springer, 2015.
[3] B. Poddar, F. Moon, and S. Mukherjee. Chaotic motion of an elastic-plastic beam. *Journal of Applied Mechanics*, vol. 55, 1988.
[4] J. J. Thomsen. Chaotic vibrations of non-shallow arches. *Journal of sound and vibration*, vol. 153, n. 2, pp. 239–258, 1992.
[5] V. Karagiozov and D. Karagiozova. Chaotic phenomena in the dynamic buckling of an elastic-plastic column under an impact. *Nonlinear Dynamics*, vol. 9, n. 3, pp. 265–280, 1996.
[6] C. Yang, A.-D. Cheng, and R. Roy. Chaotic and stochastic dynamics for a nonlinear structural system with hysteresis and degradation. *Probabilistic engineering mechanics*, vol. 6, n. 3-4, pp. 193–203, 1991.
[7] G. Luo, X. Lv, and Y. Shi. Vibro-impact dynamics of a two-degree-of freedom periodically-forced system with a clearance: diversity and parameter matching of periodic-impact motions. *International Journal of Non-Linear Mechanics*, vol. 65, pp. 173–195, 2014.
[8] H. B. Coda. An exact fem geometric non-linear analysis of frames based on position description. In *In: 17H International Congress of Mechanical Engineering. 2003, São Paulo*, 2003.
[9] M. Greco. *Analysis of contact/impact problems in nonlinear behavior structures by the finite element method. (In Portuguese)*. PhD thesis, Universidade de São Paulo, 2004.
[10] A. K. L. Kzam. *Analysis of global and local structural instability by the positional FEM with determination of critical points in the equilibrium trajectory. (In Portuguese)*. PhD thesis, Universidade de São Paulo, 2016.
[11] W. L. Fernandes, D. B. Vasconcellos, and M. Greco. Dynamic instability in shallow arches under transversal forces and plane frames with semirigid connections. *Mathematical Problems in Engineering*, vol. 2018, 2018.
[12] J. C. Simo and T. J. Hughes. *Computational inelasticity*, volume 7. Springer Science & Business Media, 2006.
[13] Z. Bažant and L. Cedolin. *Stability of structures: Elastic, inelastic, fracture and damage theories*. World Scientific Publishing Co., 2010.
[14] T. S. Parker and L. O. Chua. Chaos: A tutorial for engineers. *Proceedings of the IEEE*, vol. 75, n. 8, pp. 982–1008, 1987.